ACS APPLIED MATERIALS & INTERFACES
Research Article
www.acsami.org

Indium Oxide Thin-Film Transistors Processed at Low Temperature via Ultrasonic Spray Pyrolysis

Hendrik Faber,*[,†] Yen-Hung Lin,[†] Stuart R. Thomas,[†] Kui Zhao,[§] Nikos Pliatsikas,[⊥] Martyn A. McLachlan,[‡] Aram Amassian,[§] Panos A. Patsalas,[⊥] and Thomas D. Anthopoulos*[,†]

[†]Department of Physics and Centre for Plastic Electronics Blackett Laboratory, Imperial College London, London SW7 2AZ, United Kingdom

[‡]Department of Materials and Centre for Plastic Electronics, London Royal School of Mines, Imperial College London, London SW7 2AZ, United Kingdom

[§]Materials Science and Engineering Division of Physical Sciences and Engineering, King Abdullah University of Science and Technology, Thuwal 23955-6900, Saudi Arabia

[⊥]Department of Physics, Laboratory of Applied Physics, Aristotle University of Thessaloniki, GR-54124 Thessaloniki, Greece

Supporting Information

ABSTRACT: The use of ultrasonic spray pyrolysis is demonstrated for the growth of polycrystalline, highly uniform indium oxide films at temperatures in the range of 200−300 °C in air using an aqueous $In(NO_3)_3$ precursor solution. Electrical characterization of as-deposited films by field-effect measurements reveals a strong dependence of the electron mobility on deposition temperature. Transistors fabricated at ∼250 °C exhibit optimum performance with maximum electron mobility values in the range of 15−20 $cm^2 V^{-1} s^{-1}$ and current on/off ratio in excess of 10^6. Structural and compositional analysis of as-grown films by means of X-ray diffraction, diffuse scattering, and X-ray photoelectron spectroscopy reveal that layers deposited at 250 °C are denser and contain a reduced amount of hydroxyl groups as compared to films grown at either lower or higher temperatures. Microstructural analysis of semiconducting films deposited at 250 °C by high resolution cross-sectional transmission electron microscopy reveals that as-grown layers are extremely thin (∼7 nm) and composed of laterally large (30−60 nm) highly crystalline In_2O_3 domains. These unique characteristics of the In_2O_3 films are believed to be responsible for the high electron mobilities obtained from transistors fabricated at 250 °C. Our work demonstrates the ability to grow high quality low-dimensional In_2O_3 films and devices via ultrasonic spray pyrolysis over large area substrates while at the same time it provides guidelines for further material and device improvements.

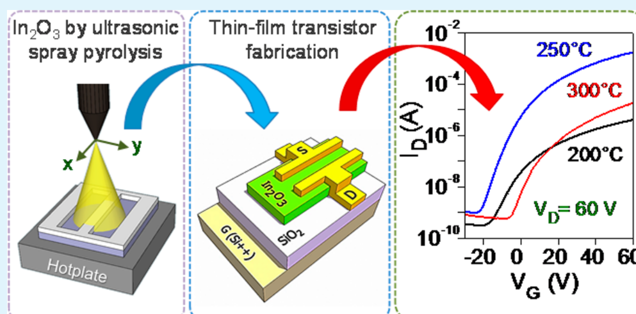

KEYWORDS: *thin-film transistors, spray pyrolysis, metal oxide, plastic electronics*

1. INTRODUCTION

Transparent oxide semiconductors have been attracting significant interest in recent years due to their potential for applications in a range of emerging optoelectronic devices including display backplanes,[1] solar cells,[2] and organic/hybrid light emitting diodes.[3] This interest is primarily driven by the continuously increasing demand for high performance semiconductors that can be processed over large areas using simple and inexpensive processing methods that are compatible with temperature-sensitive substrate materials such as polymer foils. One metal oxide semiconductor that has received significant attention over the years is the wide band gap indium oxide (In_2O_3). In its intrinsic form, In_2O_3 behaves as an electron transporting (*n*-type) semiconductor and combines a high electron mobility (up to 160 $cm^2 V^{-1} s^{-1}$ for single crystals[4]) with high optical transparency. Additionally, indium (In) is often employed as a key component in high performance ternary/quaternary oxide semiconducting systems in which the overlap of its large spherical 5s orbitals provides the foundation for effective charge transport, even in disordered systems.[5]

Indium oxide can be processed by a diverse range of vapor phase techniques such as sputtering,[6] reactive thermal evaporation,[7] and pulsed laser deposition.[8] Potentially inexpensive and high throughput solution-based deposition techniques such as spin-casting, inkjet printing[9] and spray pyrolysis (SP)[10] have also been demonstrated with some success. Among these, SP represents one of the simplest and most scalable deposition methods demonstrated to date for the growth of a variety of metal oxide materials and active devices such as thin-film transistors.[11−15] The SP process is simple and

Received: October 18, 2014
Accepted: December 10, 2014
Published: December 10, 2014

ACS Publications © 2014 American Chemical Society

DOI: 10.1021/am5072139
ACS Appl. Mater. Interfaces 2015, 7, 782−790

is based on the atomization of the precursor solution and the direction of the mist toward a heated substrate where chemical conversion of the precursor to the final material takes place upon contact. Among the several key process parameters such as precursor solution feed rate, solvent, precursor and precursor concentration in the solution, as well as hotplate temperature, the droplet size has been shown to have a direct impact on the film structure and chemistry. A narrow distribution with small droplets is generally favored[16] and this can be more easily achieved using an ultrasonic atomization process rather than, for example, with gas-assisted atomizers (airblast atomizers etc.). Over large areas, the SP process can be material efficient (only about 20 μL cm^{-2} in our setup) and, contrary to e.g. spin coating, a direct patterning is possible using stencil masks[15] or a gas flow assisted deposition as in aerosol jet printing.[17]

Despite its potential, however, use of SP has so far been limited to processing temperatures in excess of 300−400 °C. This high temperature requirement is primarily dictated by the decomposition temperature of the precursor molecules employed. As such, significant research efforts in recent years have been devoted to the study of precursor compounds with lower decomposition temperatures. Among the studied materials are compounds such as $InCl_3$,[18−24] indium acetylacetonate,[25] and indium nitrate. Of particular relevance to this work is the recent use of indium nitrate for the growth of high quality In_2O_3 layers and active devices at temperatures in the range 200−300 °C.[9,26−28]

Here we explore the use of ultrasonic spray pyrolysis in combination with the low conversion temperature precursor indium nitrate hydrate ($In(NO_3)_3 \cdot H_2O$) for rapid and large-area deposition of high quality In_2O_3 films and devices at temperatures in the range 200−300 °C. Electrical field-effect measurements reveal that films and devices grown at 250 °C exhibit optimum performance with maximum electron mobility values and channel current on/off ratios exceeding 20 cm^2/(V s) and >10^6, respectively. Deposition of In_2O_3 films at either higher or lower deposition temperatures is found to degrade the device's operating characteristics dramatically. Through extensive material analysis using a range of complementary techniques we show that the observed performance degradation at these higher and lower temperatures is directly linked to increased film porosity (i.e., reduced density) and the presence of an increased amount of hydroxyl groups. Importantly, control experiments reveal that transistors fabricated by ultrasonic spray pyrolysis outperform devices prepared via spin-casting in air, hence highlighting the advantages associated with this simple, rapid and highly scalable deposition method. Most importantly, analysis of In_2O_3 films grown at 250 °C by high resolution transmission electron microscopy (HR-TEM) reveals that as-grown layers are extremely thin (~7 nm) and composed of long-range epitaxial-like crystalline In_2O_3 domains. The findings highlight the tremendous capabilities of the SP method to grow low-dimensional layers with chemical and structural quality resembling that of films deposited by highly sophisticated techniques such as metal organic chemical vapor deposition (MOCVD), etc. Understanding of the reaction kinetics during film growth by SP is expected to lead to further improvements in film's stoichiometry/morphology and potentially device performance. This work is the first to demonstrate the technological potential of SP as a viable deposition method for the growth of high quality In_2O_3 films and field-effect transistors at low temperatures.

2. EXPERIMENTAL SECTION

2.1. Transistor Fabrication and Characterization. Doped silicon (Si^{++}) wafers with a 400 nm thick thermally grown SiO_2 layer acting as the common gate and gate dielectric, respectively, were employed for the fabrication of bottom-gate, top-contact transistors. Prior to indium oxide deposition, the Si^{++}/SiO_2 substrates were cleaned by sequential ultrasonication in deionized water, acetone, and IPA, with each step lasting for approximately 10 min. Substrates were subsequently exposed to atmospheric pressure UV/ozone for 10 min at room temperature. Solutions of 30 mg/mL indium nitrate hydrate ($In(NO_3)_3 \cdot H_2O$) in deionized water were used as the precursor for the growth of the indium oxide layers. Ultrasonic spray pyrolysis was performed using a fully automated Sono-Tek Corporation coating system. The deposition process consisted of four spraying steps with a 2 min resting time in between coating steps, with the entire deposition lasting 10 min (deposition area 15 × 10 cm). During processing, the deposition temperature (T_D) was set to a fixed value in the range 200−300 °C. The resulting film thickness was found to vary with the deposition temperature. To reduce unwanted effects such as fringing currents around the channel and lateral gate leakage currents, all indium oxide films were patterned using stencil masks. Device fabrication was completed with the thermal evaporation of aluminum source-drain (S-D) contacts in high vacuum (10^{-6} mbar) using shadow masks. Transistor characterization was carried out in nitrogen atmosphere with the samples maintained at room temperature using an Agilent B2902A parameter analyzer. The field-effect electron mobility was extracted from the saturation regime using the gradual channel approximation according to

$$\mu_{sat} = \frac{L}{WC_i} \frac{\partial^2 I_{D(SAT)}}{\partial V_G^2} \quad (1)$$

Here, W is the channel width, L the channel length, $I_{D(SAT)}$ the channel current in saturation, and C_i the geometric capacitance of the gate dielectric employed.

2.2. Material Characterization Techniques. The surface morphology was investigated using atomic force microscopy (AFM) in intermittent contact mode using an Agilent 5500AFM system. UV−vis transmittance and reflectance spectra of as-deposited indium oxide films on quartz substrates were recorded with a Shimadzu 2600 UV−vis spectrophotometer equipped with an ISR-2600Plus integrating sphere.

Measurements of X-ray diffraction (XRD) in Bragg−Brentano geometry and grazing incidence XRD (GIXRD) in asymmetric geometry were performed using a Bruker D8-ADVANCE X-ray diffractometer equipped with Cu X-ray tube (at 40 kV and 40 mA), parallel beam optics (Göbel mirror), and a solid state linear strip detector (Bruker's LynxEye). Contributions of the substrates to the XRD/GIXRD signals were evaluated and subtracted by measuring the back sides of the samples. Crystallite size analysis was carried out using the Scherrer method.

The X-ray photoelectron spectra (XPS) were acquired in a KRATOS Axis Ultra DLD system equipped with a monochromated Al Kα X-ray source. The XPS measurements were acquired using 20 eV pass energy.

High resolution transmission electron microscopy (HR-TEM) measurements were acquired using a Titan 80−300 Super Twin microscope (FEI Company) operating at 300 kV, equipped with a US4000 charged couple device (CCD) camera (Gatan Inc.). A CCD camera (Model: US1000, Gatan Inc.) was used to record the HR-TEM images. Samples were prepared in a focused ion beam (FIB; Helios 400s, FEI) equipped with a nanomanipulator (Omniprobe, AutoProbe300) using the lift-out method. Electron beam assisted carbon and platinum deposition was performed on the sample surface to protect the thin film surface against the ion beam bombardment during ion beam milling. A Ga ion beam (30 kV, 9 nA) was first used to cut the sample from the bulk (30 kV, 9 nA), after which it was attached to a Cu grid using a lift-out method. The sample was subsequently thinned down to ca. 50 nm thickness (30 kV, 93 pA) and cleaned (2 kV, 28

DOI: 10.1021/am5072139
ACS Appl. Mater. Interfaces 2015, 7, 782−790

pA) to get rid of areas of the sample damaged during the thinning process.

3. RESULTS AND DISCUSSION

3.1. Film Deposition and Characterization. Figure 1a displays the atomic force microscopy (AFM) images of the surfaces of several In_2O_3 films grown at temperatures (T_D) in the range 200−300 °C at two different magnifications (5 × 5 μm^2 and 1 × 1 μm^2). It can be seen that the surface topography of the films depends strongly on T_D. This effect is better illustrated in Figure 1b where the root-mean-square (rms) surface roughness of each film is plotted versus T_D, and in Figure 1c where the height distributions are plotted for indium oxide films grown at different temperatures. Films grown at 200 °C appear to be highly nonuniform and thick (100−400 nm) and exhibit extremely high surface roughness with typical rms values of ∼38 nm. On the other hand, films deposited at $T_D \geq$ 250 °C are found to be extremely smooth with surface roughness rms ≤ 1 nm. These differences are most likely attributed to the different reaction kinetics responsible for the formation of the indium oxide layer during growth. To this end, a higher T_D is expected to result in accelerated chemical reactions, thus leading to more compact films whereas a lower T_D to lower kinetics and rougher films. Interestingly, even at higher T_D's the films' surfaces bear spherical features (better observed in the 5 × 5 μm^2 images in Figure 1a) that are believed to be the residual marks of individual droplets impinging on the substrate surface, possibly in a process similar to a transition boiling film formation as described in ref 29. There, the droplets reach the substrate surface and then form a cushion of vapor underneath them, allowing for a film forming process from the vapor phase. The droplets then touch the substrate when the unstable vapor cushion collapses, leading to

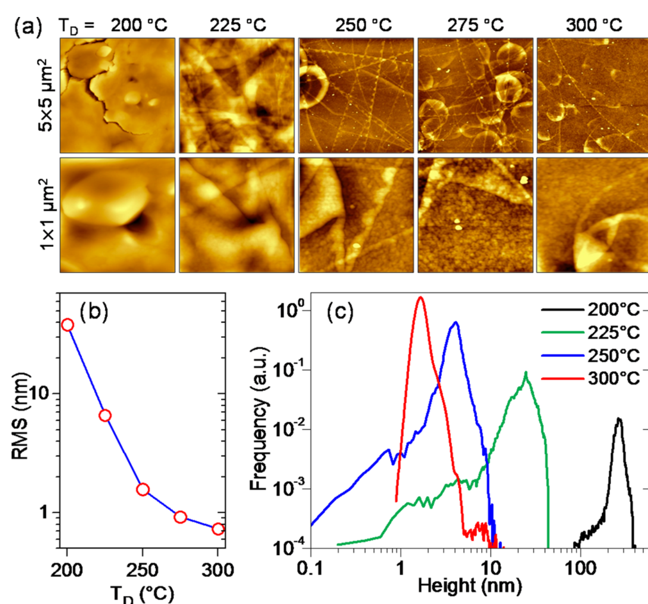

Figure 1. (a) AFM topography images of indium oxide films deposited at different temperatures. The top row shows 5 × 5 μm^2 scans whereas the bottom row shows higher magnification 1 × 1 μm^2 scans. (b) Evolution of the root-means-square (rms) of the surface roughness of indium oxide films as a function of T_D. (c) Height distribution extracted from the AFM topography images for several indium oxide films grown at different temperatures in the range 200−300 °C.

the formation of spherical features. Although visible by means of AFM, these features are themselves extremely flat, thereby not deteriorating the overall film roughness/continuity. Similarly, electron transport in these films, evaluated via field effect measurements, appears to be independent of these nanoscale topographical features with the most critical parameter remaining the growth temperature and physical continuity of the as-grown films (see section 3.4).

The film thickness of the deposited oxide is also found to decrease with increasing deposition temperature and reducing precursor solution molarity. This may be unexpected, considering that the same volume of precursor solution was sprayed on the substrates at each temperature. However, similar results were reported for spray pyrolysis of ZnO from zinc acetate by Krunks et al.[30] In the latter study, the authors argued that the increased heat convection above the hotplate at a high T_D is repelling a fraction of droplets away from the substrate. This mechanism would also be consistent with the decrease in occurrence and size of the residual droplet marks observed in larger (5 × 5 μm) AFM scans of films deposited at T_D > 250 °C. Finally, close examination of the AFM images, especially for the 250 °C sample, shows signatures of structural regularity as would be expected for a polycrystalline film. However, due to the limited AFM resolution, these microstructural features could not be fully resolved by tapping-mode scanning probe technique with limited lateral resolution and required more advanced microanalysis tools, as will be discussed in section 3.4 where HR-TEM microscopy is employed to elucidate the thickness and crystallinity of the as-grown films.

3.2. Optical Characterization of In_2O_3 Films Grown by Spray Pyrolysis. The optical properties of indium oxide films grown by spray pyrolysis on quartz substrates at different T_D values were investigated. Figure 2 displays the transmittance and reflectance measurements obtained for indium oxide films grown at three different temperatures. All as-grown films are found to be highly transparent in the visible part of the electromagnetic spectrum, with an average transmittance in the range 87−91%. A sharp drop in film's transmittance is observed in the UV range as expected for a wide band gap semiconductor due to interband absorption. The values of the optical band gap, extracted via Tauc plot analysis (see the Supporting Information, Figure S1), are between 3.77 and 3.81 eV. These numbers are slightly higher than the typical band gap values reported indium oxide films grown by spray pyrolysis (3.5−3.7

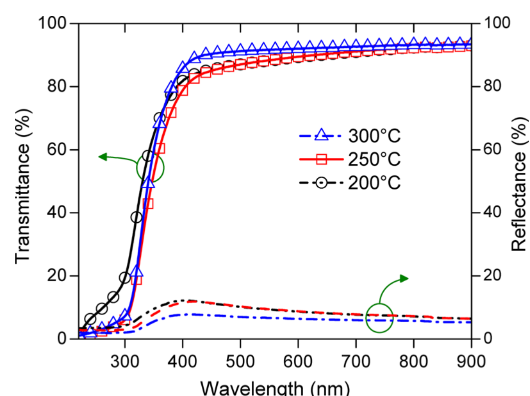

Figure 2. (a) Specular transmission and reflection spectra of indium oxide films grown by ultrasonic spray pyrolysis at temperatures in the range 200−300 °C.

DOI: 10.1021/am5072139
ACS Appl. Mater. Interfaces 2015, 7, 782−790

eV)[20,21,23−25,31] but in good agreement with values measured for single crystal In_2O_3.[32] As the deposition temperature increases, the films appear less reflective. This can be explained by the change in surface morphology, since rougher surfaces with coarse features can lead to increased off-specular light scattering and hence to higher reflectance while smoother surfaces tend to be less scattering and do not suffer from off-specular scattering losses.

3.2. Grazing Incident X-ray Diffraction and X-ray Diffused Scattering Measurements. As-grown indium oxide films were characterized via X-ray diffraction (XRD) in Bragg−Brentano geometry and grazing incidence XRD (GIXRD) measurements. The XRD survey scans are shown in Figure S2 (Supporting Information). All three investigated samples show five distinct peaks at the same 2θ values, regardless of their deposition temperature. The peak positions identify the thin films as crystalline, cubic In_2O_3 belonging to the space group $Ia\overline{3}$. There are no significant variations between the obtained diffraction patterns and the reference powder diffraction file 06-0416 (JCPDS-PDF 06-0416). Analysis of the mean grain size was also carried out using the Scherrer method using

$$L_g = \frac{\lambda}{\text{fwhm}\cos\theta_B} \tag{2}$$

Here, θ_B is the Bragg angle and fwhm is the full width of half-maximum of the (222) peak (Figure 3a). For deposition temperatures of 200, 250, and 300 °C, the resulting mean crystallite sizes were calculated to be 8.1, 9.3, and 8.4 nm, respectively. The largest grains were therefore obtained at a deposition temperature of 250 °C. However, the overall variation is very small and in terms of grain size alone, the deposition temperature is therefore not considered to be critical.

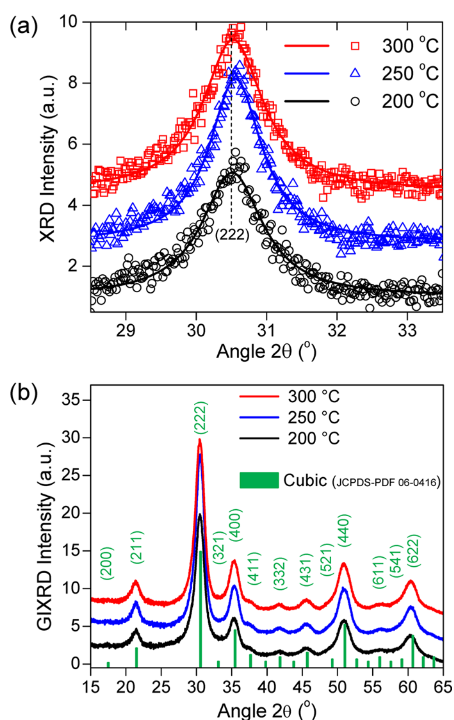

Figure 3. (a) Close-up view of the (222) XRD peak along with the Lorentzian fits (solid lines) used to determine the grain size for three indium oxide films grown at different temperatures. (b) GIXRD patterns of the same In_2O_3 films. The green markers represent the peak positions of the cubic indium oxide powder reference. In both cases, the patterns are vertically moved for better visibility and represent data after subtraction of substrate contributions.

As the weaker peaks of the powder diffraction reference could not be resolved, additional grazing incidence XRD experiments were carried out, using an angle of incident $\alpha = 2°$. This geometry increases substantially the signal-to-noise ratio (due to the longer path of the X-rays into the film) but it has poorer focusing conditions of the diffracted beam to the detector, resulting in slightly broader peaks. Compared to the XRD data, the GIXRD diffraction patterns, shown in Figure 3b, successfully resolve an increasing number of peaks. Again, all features can be matched to the indium oxide powder reference file (see the Supporting Information, Figure S3), hence confirming the presence of a cubic In_2O_3 crystal structure.

X-ray diffused scattering (XDS) measurements were carried out in order to study the density of the as-deposited indium oxide films (see the Supporting Information, Section S4, Figure S4). Although the XDS technique is better suited to study rough films than, for example, X-ray reflectivity,[33−35] measurements performed on indium oxide films grown at $T_D = 200$ °C did not yield sufficient signal for analysis to be performed, indicating the sample roughness was still too high. Samples grown at 250 °C were found to be substantially denser (ρ = 4.75 g cm^{-3}), as compared to film grown at 300 °C (ρ = 3.25 g cm^{-3}) (Figure S4, Supporting Information). Both density values are lower than that of crystalline In_2O_3 (ρ = 7.179 g cm^{-3}) but are close to the density of indium hydroxide ($In(OH)_3$), which is ρ = 4.38 g cm^{-3}. This suggests that chemical conversion of the initial $In(NO_3)_3$ precursor to In_2O_3 is not entirely completed for either temperature and significant residues of $In(OH)_3$ most likely still remain inside the as-grown films. On the basis of this analysis, we conclude that the indium oxide films grown by spray pyrolysis at T_D values in the range 250−300 °C are rather porous and consist of a mixture of In_2O_3 and $In(OH)_3$. This is an important finding because further improvement in electronic properties of the films would require the In_2O_3 phase to be increased while the $In(OH)_3$ to be reduced or completely eliminated.

3.3. Elemental Composition and Chemical Bonding States Analysis by XPS. The surface elemental composition of as-deposited indium oxide films on Si wafers was determined by X-ray photoelectron spectroscopy (XPS). The wide scan spectra are presented in Figure 4 and show the characteristic photoelectron lines of In, O, adventitious C, Si (due to the presence of pinholes in the films), and N (due to incomplete precursor conversion). The elemental compositions, determined under consideration of the In 3d, O 1s, N 1s, C 1s, and Si 2p peaks, are listed in Table 1. In all cases, the [O]/[In] ratio is found to be higher than the nominal value of 1.5 for In_2O_3 due to a combination of factors such as the existence of oxygen-rich $In(OH)_3$, adventitious O, and the contribution of oxygen from exposed SiO_2 regions (substrate material) due to pinholes in the film. The Si contribution is increasing with increasing T_D, which is in accordance with the trend toward a reducing film thickness and the formation of pinholes. Residual nitrogen (N) due to an incomplete conversion reaction was detected only for samples deposited at 200 and 300 °C, but not in films grown at 250 °C.

The process of In_2O_3 formation during spray pyrolysis needs to be considered as interplay of different factors such as the

DOI: 10.1021/am5072139
ACS Appl. Mater. Interfaces 2015, 7, 782−790

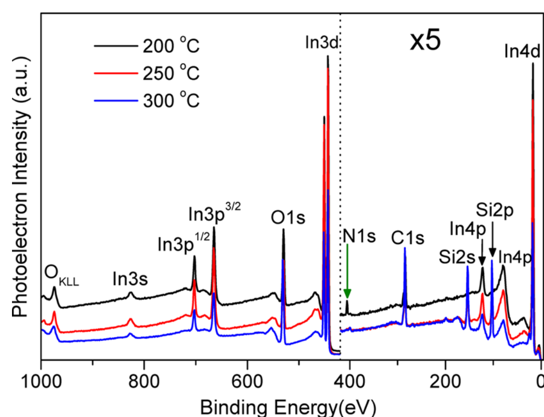

Figure 4. XPS survey scan wide scan spectra obtained for three In_2O_3 films grown at 200, 250, and 300 °C. The legends indicate the assignment of the corresponding photoelectron and Auger lines.

number and volume of droplets reaching the surface and their spreading behavior, the kinetics of the conversion reaction, and/or the rate of solvent evaporation. With that in mind, given our material system and process parameters, the deposition temperature of 250 °C appears to provide the best conditions for In_2O_3 growth, as it combines the highest percentage of precursor conversion with the formation of denser and more uniform films. Although serendipitous, this is an important finding as it enables the growth of high quality indium oxide films at temperatures compatible with certain plastic substrates (e.g., polyimide). Therefore, further optimization of any of the deposition parameters may lead to significant improvements in the film's stoichiometry and potentially the resulting charge transporting characteristics.

The high resolution XPS spectra were measured (Figure 5) and analyzed to gain more information about the types of chemical bonds present within the spray deposited indium oxide films. Unlike the indium spectra, which do not exhibit significant changes between In−O and In−OH bonds,[36] the O 1s spectra are a very sensitive indicator of bonds between oxygen and other elements and it can thus be used to distinguish between different contributions to the overall oxygen signal recorded in the wide range XPS scans. The O 1s spectra corresponding to indium oxide films deposited at 200, 250, and 300 °C are summarized in Figure 5. In all cases, the O 1s envelope can be deconvoluted to three individual peaks located at 529.5 eV (In−O bonds in In_2O_3), 530.2 eV (O adsorbates on the surface), and 532 eV (water and In−OH bonds).[37] The sample grown at 200 °C exhibits high contributions related to oxygen adsorbates and In−OH bonds, but only a small amount of signal intensity relates to In−O bonds. Less than 20 at. % of oxygen is thus present in the In_2O_3 phase, indicating that 200 °C is not sufficient for an effective precursor conversion reaction to occur. Sample grown at 250 °C still shows hydroxyl related contributions, but features the highest amount of In−O bonds. Finally, deconvolution of the O 1s spectrum for the 300 °C films

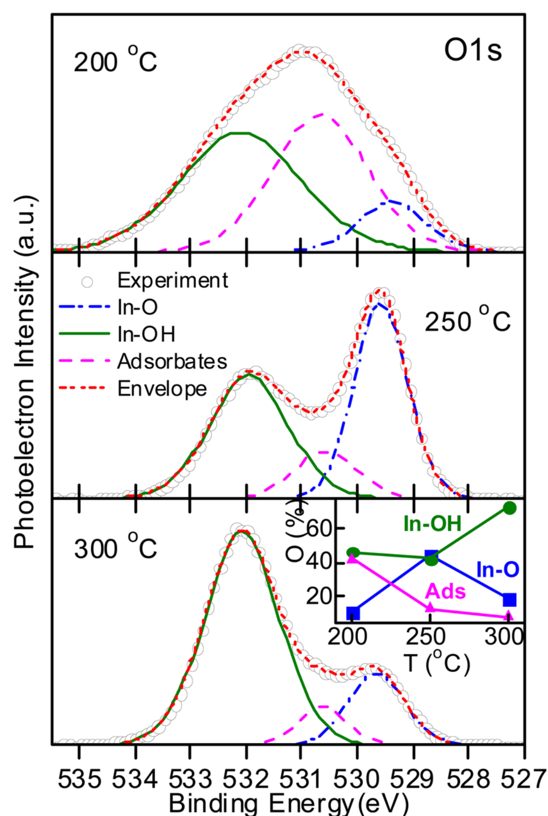

Figure 5. XPS O 1s high resolution spectra (circles and solid line envelope) for indium oxide films grown at 200, 250, and 300 °C (top-down). Together with the experimental data, plots illustrating the deconvolution into In−O (dash dot line), O adsorbates (dash line), as well as In−OH peaks (long dash dot dot line), are also shown. The inset in the 300 °C plot displays the contributions of the respective peaks.

reveals that the major contribution comes from the In−OH bonds and to a lesser degree from the In−O and O-adsorbate bonds. The reason for this may be the fact that at this elevated temperature the rate of solvent evaporation is significantly faster, thus kinetically hampering complete conversion of the indium nitrate precursor, which in turn prevents formation of dense In_2O_3 films.

On the basis of these results, we conclude that indium oxide films grown at 200 °C, 250 and 300 °C are all characterized by incomplete precursor conversion, the degree of which depends strongly on T_D. Of particular importance is the finding that In_2O_3 films grown at T_D = 250 °C show the highest amount of In−O bonds that can directly be linked to a highest degree of precursor conversion and thus are expected to exhibit optimum electrical characteristics, in terms of charge carrier mobility, as they combine key favorable attributes such as the largest grain size, a reduced amount of hydroxyl groups and a lower film porosity. Finally, these findings also hint at the possibility for further improvements of process conditions aiming toward more complete precursor conversion and the formation of films

Table 1. Results of XPS Surface Elemental Analysis of Indium Oxide Films Grown at Different Temperatures

temperature (°C)	[In] (% at)	[O] (% at)	[N] (% at)	[Si] (% at)	[C] (% at)	[O]/[In]
200	26.9	53.3	1.8	0.0	18.0	1.98
250	25.3	49.8	0.0	8.4	16.5	1.96
300	12.6	48.7	0.4	16.7	21.6	3.87

DOI: 10.1021/am5072139
ACS Appl. Mater. Interfaces 2015, 7, 782−790

with significantly increased density and/or crystallinity. A possible option for that purpose is the usage of a self-energy generating precursor containing a fuel and an oxidizer component as demonstrated in the pioneering work by Kim et al.[26]

3.4. Indium Oxide Thin-Film Transistors Grown by Ambient Ultrasonic Spray Pyrolysis. To study the impact of the processing conditions and film stoichiometry on the charge transport properties of as-grown In_2O_3 layers, we fabricated thin-film transistors based on the bottom-gate, top-contact (BG-TC) architecture (Figure 6a). Figure 6b displays a set of representative transfer characteristics measured in saturation (drain voltage (V_D) = 60 V) for several transistors fabricated in air at temperatures in the range 200−300 °C. The complete sets of the transfer and output characteristics of these transistors are shown in Figure S5 (Supporting Information), whereas Table S2 (Supporting Information) summarizes the key operating parameters. As can be seen, all transistors independent of processing temperature exhibit electron transporting (*n*-channel) characteristics with clear channel current (I_D) saturation [for $V_D \geq (V_G - V_T)$], minor operating hysteresis between forward and reverse gate voltage sweeps and Ohmic-like injection characteristics as evident from the linear dependence of I_D versus V_D at low voltages. Based on these results, it can be concluded that the transistor performance is primarily determined by the deposition temperature of the In_2O_3 layer. This is better illustrated in Figure 6c where the electron mobility (μ_{SAT}), measured in saturation, for several transistors (error bars included) is plotted as a function of T_D (square symbols). Devices fabricated at 200 °C exhibit poor performance, with a mean electron mobility value of ~0.01 $cm^2\ V^{-1}\ s^{-1}$. A dramatic increase of μ_{SAT} to >16 $cm^2\ V^{-1}\ s^{-1}$ is obtained for transistors prepared at T_D = 250 °C. An increase of T_D to ≥300 °C, and maintaining the same film deposition procedures, leads to a significant reduction in μ_{SAT} to ≤0.4 $cm^2\ V^{-1}\ s^{-1}$. This dramatic drop in electron mobility may be partly attributed to the reduced thickness of the semiconducting film and associated layer discontinuities. To investigate this further we deposited In_2O_3 films using 25 spraying cycles (instead of 4) and evaluated the electron mobility of the resulting transistors. Despite the presence of significantly thicker oxide films, the electron mobility remained relatively low and on the order of 3 $cm^2/(V\ s)$. Therefore, we can conclude that although the active layer thickness does play a role, it cannot be held fully responsible for the dramatic reduction in electron mobility observed in devices grown at 300 °C. Following a similar trend, the on/off ratio of the channel current reaches a maximum of ~7×10^6 for In_2O_3 transistors prepared at T_D = 250 °C, whereas lower or higher deposition temperatures lead to smaller on/off ratios that are typically in the range 10^4−10^5. Worth mentioning is that all devices exhibit stable operation even after storage for 16 days in dry nitrogen (Figure 6b (circles)).

On the basis of the results presented so far, it can be argued that the high μ_{SAT} measured for devices prepared at T_D = 250 °C is most likely attributed to the improved In_2O_3 morphology and stoichiometry because films grown at this temperature are more homogeneous (Figure 1) and significantly denser (Figure S4, Supporting Information). Furthermore, residual nitrogen (N), which is known to act as an acceptor in In_2O_3,[27,38] is removed more efficiently at elevated temperatures (detected in the XPS spectrum in Figure 4), thus improving the transport characteristics of the transistors. The maximum μ_{SAT} obtained for devices prepared at T_D = 250 °C can thus be directly linked to a combination of improved chemical and structural characteristics of the In_2O_3 films including the absence of residual N, relatively low concentration of In−OH groups, high concentration of In−O bonds, largest crystalline grain size and therefore reduced number of grain boundaries, highest film density, and finally, film continuity.

For indium oxide films grown at 300 °C, the [O]/[In] ratio is found to deviate strongly from the stoichiometric value of 1.5 due to high contributions from the In−OH and low contribution from the actual In−O bonds. This increased concentration of In−OH groups together with the reduced film density, are believed to be the two main reasons for the significant reduction in the field-effect electron mobility measured. When the films are subjected to a postannealing step at 300 °C no significant improvement in devices'

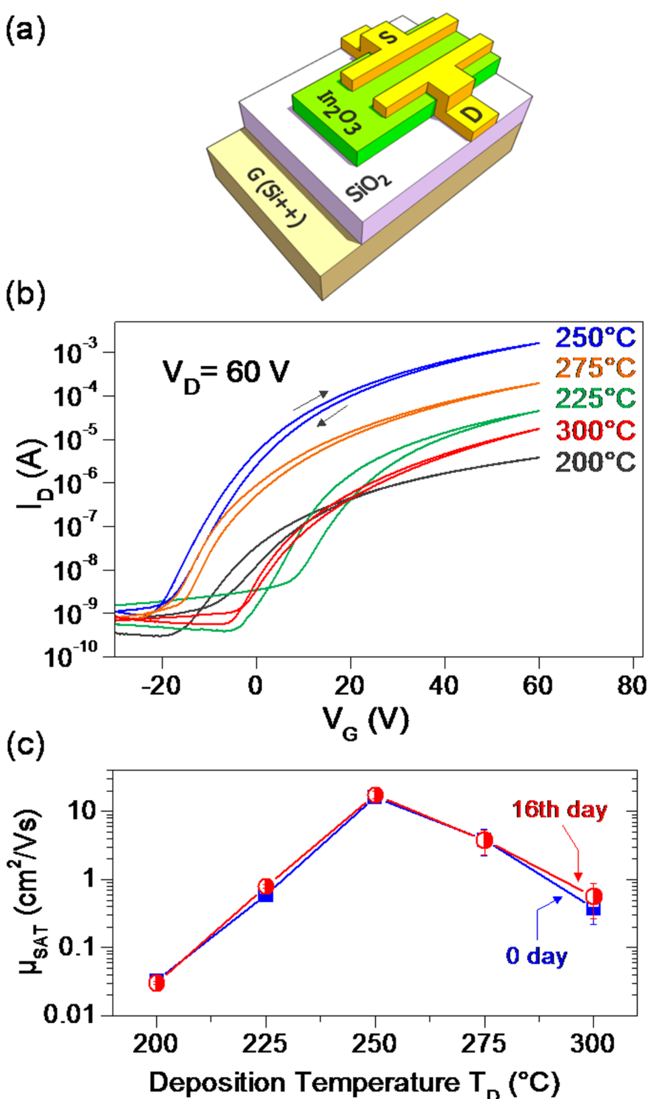

Figure 6. (a) Schematic of the bottom-gate, top-contact transistor architecture employed for the field-effect measurements. (b) Transfer characteristics of indium oxide transistors fabricated on Si/SiO_2 wafers processed at temperatures in the range 200−300 °C. All devices featured channel widths (W) and lengths (L) of W = 1000 μm and L = 100 μm, respectively. (c) Plot of electron mobility versus deposition temperature (T_D) for as-prepared devices measured immediately after fabrication (day 0), and after 16 days of storage in dry nitrogen.

DOI: 10.1021/am5072139
ACS Appl. Mater. Interfaces 2015, 7, 782−790

performance is observed. This suggests that the films' morphology is the key limiting factor to electron transport. However, further work would be needed in order to identify the role of reaction kinetics and its impact on the film's morphology (e.g., crystallinity, density of grain boundaries) and electron transporting characteristics.

Qualitatively similar temperature dependences of the electron mobility in In_2O_3 films deposited by spray pyrolysis using indium acetylacetonate and $InCl_3$ precursors at different temperatures have been reported in literature.[21,23,25] However, in these previous studies, emphasis was placed on analyzing the Hall electron mobility, as opposed to field-effect mobility, where the electron mobility modulation (versus T_D) was found to be far less pronounced and was attributed to changes in the preferred crystalline orientation of In_2O_3. The latter effect may also play an important role on the electron transporting characteristics of our transistors and will be the subject of future investigations.

To gain a better understanding of the microstructural properties of In_2O_3 films grown at 250 °C, we have performed cross-sectional HR-TEM measurements on the channel region of an actual transistor. Figure 7a−c displays the lower to higher magnification HR-TEM micrographs of the In_2O_3 channel layer grown on SiO_2 by ambient ultrasonic spray pyrolysis at 250 °C. Surprisingly, the In_2O_3 layer is found to be highly textured, polycrystalline, and ultrathin, with an average thickness of ∼7 nm. Despite the fact that the In_2O_3 films were grown on amorphous SiO_2, the HR-TEM micrographs reveal the presence of crystalline domains up to 60 nm in lateral dimensions. However, randomly oriented crystalline domains are also observed along the interface, in agreement with the powder-like X-ray diffraction patterns measured (Figure S3, Supporting Information), indicating the film is not perfectly textured. The lattice spacing of 0.36 nm, indicated in the high magnification micrograph of Figure 7c, matches well with the (220) crystal plane of the expected body centered cubic structure of In_2O_3. The remarkably high crystallinity and long-range order in these ultrathin In_2O_3 films is rather surprising if one takes into account the amorphous substrate, the low deposition temperature, as well as the ambient atmosphere conditions in which the spray pyrolysis technique is used.

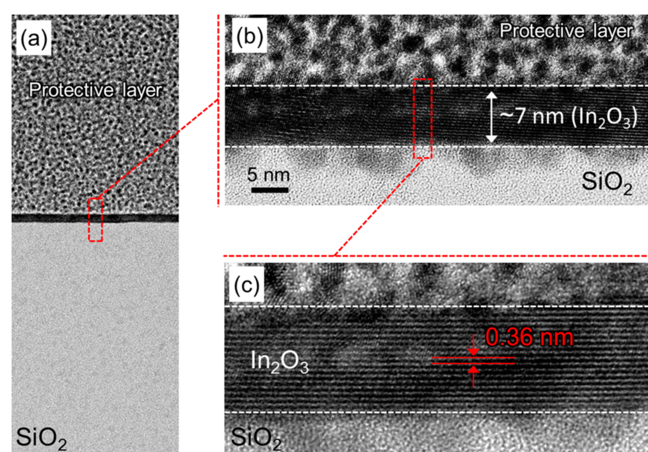

Figure 7. High resolution transmission electron micrographs (HR-TEM) of the channel SiO_2/In_2O_3 cross section. Panel a shows the low magnification cross-section micrograph of the FIB milled section whereas panels b and c show the medium and high magnification micrographs.

Although scientifically interesting, the characteristically low-dimensional nature of the semiconducting channel may have a negative impact on the overall ambient stability of the device primarily due to physisorption of atmospheric polar molecules (e.g., oxygen, water) onto the surface of the ultrathin In_2O_3 layers. Presence of such species in close proximity to the semiconducting channel may degrade the performance of the transistors both in terms of operating hysteresis and electron carrier mobility. Therefore, device encapsulation may well be required in order to ensure stability under realistic operating conditions. To this end, a detailed study of the device operating stability, including bias stress and the impact of atmospheric oxidants, is currently under way and will be reported in the future as it is beyond the scope of this work.

Using the electron mobility as the main figure of merit the performance level of In_2O_3 transistors prepared at 250 °C reported in this study is comparable or even surpasses recently reported values for solution-processed indium oxide transistors based on similar device architectures.[9,18,19,26−28] A potentially important advantage of spray pyrolysis, as opposed to conventional solution-based methods such as spin-coating, is that the former technique can easily be adapted to a continuous deposition process with minimal material wastage and high deposition throughput. Therefore, the present work can be seen as a significant step toward scalable, low temperature manufacturing of high performance metal oxide opto/electronics.

3.5. Low-Voltage In_2O_3 Transistors grown by Ultrasonic Spray Pyrolysis.

Despite the high mobility characteristics of the In_2O_3 transistors shown in Figure 6, all devices operate at high voltages (typically in the range 50−80 V) and hence consume much power. The latter is primarily determined by the 400 nm thick SiO_2 gate dielectric employed and its relatively low dielectric constant (∼3.9). In an effort to lower the operating voltage, and hence the overall power consumption of In_2O_3 transistors, we have replaced the SiO_2 dielectric layer with a solution-processed high κ metal oxide dielectric composed of a bilayer AlO_X/ZrO_2 (see the Experimental Section and inset in Figure 8a). The entire dielectric deposition process was performed at low temperature using an ultraviolet light-assisted chemical conversion process described previously,[39] followed by the deposition of In_2O_3 layers via spray pyrolysis at 250 °C. A representative set of transfer and output characteristics measured are shown in Figure 8. Due to the high geometrical capacitance of the bilayer AlO_X/ZrO_2 dielectric (∼250 nF cm^{-2}), as-prepared transistors operate at significantly reduced voltages (∼|2 V|) and exhibit low turn-on and threshold voltages (V_{TH}) of ∼0 and ∼0.4 V, respectively. Compared to the SiO_2-based In_2O_3 transistors, both the current on/off ratio and electron mobility of the low voltage devices are consistently lower, with typical values on the order of 10^2 and ∼1 cm^2 V^{-1} s^{-1}, respectively. Despite the reduced level of performance, however, the results demonstrate the possibility of fabricating low voltage/power In_2O_3 transistors from solution over large area substrates at plastic-compatible temperatures without any special precautions. Further processing and material chemistry developments and optimization are most certainly required to lead to additional improvements of the operating characteristics and will be the subject of future studies.

DOI: 10.1021/am5072139
ACS Appl. Mater. Interfaces 2015, 7, 782−790

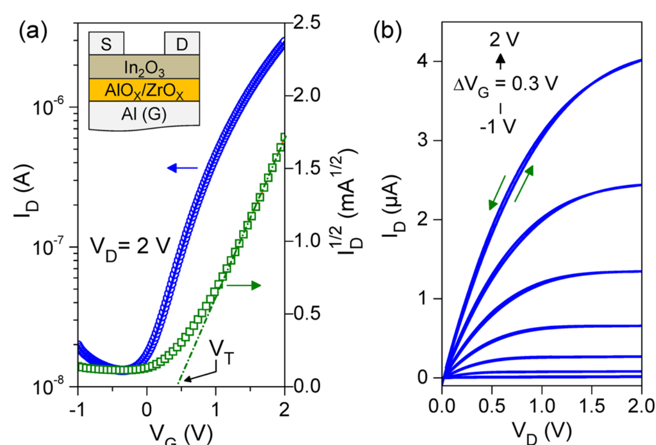

Figure 8. (a) Transfer characteristic of a representative low operating voltage In_2O_3 transistor fabricated at 250 °C. The transistor structure features a bilayer AlO_X/ZrO_2 dielectric and symmetric Al source-drain electrodes. The channel width (W) and length (L) of this particular transistor were 1000 and 100 μm, respectively. (b) Corresponding output characteristics measured from the same transistor.

4. CONCLUSIONS

Indium oxide thin-film transistors were successfully fabricated using the ambient ultrasonic spray pyrolysis method in combination with a low decomposition temperature (200–300 °C) indium nitrate-based precursor solution. Although all as-grown indium oxide films were found to consist of a mixture of crystalline In_2O_3 and $In(OH)_3$, best device performance was achieved at the intermediate deposition temperature of 250 °C. Best performing transistors showed to be very reproducible with a mean electron mobility value of ~16 $cm^2\ V^{-1}\ s^{-1}$ and typical channel on/off ratios exceeding 10^6. Extensive material and device characterization suggest that the presence of a reduced concentration of In–OH groups together with the formation of denser films at 250 °C, are the two primary reasons for the improved transistor performance observed. However, other effects such as film continuity, thickness, and density of grain boundaries may well play important roles and are currently the subjects of ongoing investigations. Surprisingly, In_2O_3 films grown at 250 °C are found to be highly continuous, smooth (surface roughness rms <2 nm), extremely thin (~6–8 nm), and highly crystalline. The potential of combining the sprayed In_2O_3 layers with solution processed AlO_X/ZrO_2 high κ dielectrics for the development of low operating voltage (<2 V) transistors was also successfully demonstrated. The combination of ambient ultrasonic spray pyrolysis with the aqueous-based indium nitrate precursor chemistry allows straightforward up-scaling of the processing of high mobility In_2O_3 layers at low temperatures that are even compatible with temperature sensitive substrates such as plastic. We are confident that further device optimization may be achieved through improved processing protocols and by establishing a better understanding of the structure–property relationship in these ultrathin layers of In_2O_3.

■ ASSOCIATED CONTENT

Supporting Information

Tauc analysis, further XRD and XDS investigations, as well as representative transfer and output characteristics of In_2O_3 TFTs processed at different temperatures. This material is available free of charge via the Internet at http://pubs.acs.org

■ AUTHOR INFORMATION

Corresponding Authors

*Prof. T. D. Anthopoulos. E-mail: t.anthopoulos@ic.ac.uk.
*Dr. Hendrik Faber. E-mail: h.faber@imperial.ac.uk.

Author Contributions

H.F, Y.-H.L, S.R.T., and T.D.A. designed the experiments, performed the AFM, TFT, UV–vis measurements, and wrote the relevant parts of the paper. K.Z., A.A., and M.A.M., performed the TEM measurements and the relevant data analysis, and assisted with the writing of the paper. N.P. and P.A.P. performed the XPS and XRD measurements and the data analysis and wrote the relevant parts of the paper. All authors have given approval to the final version of the paper.

Notes

The authors declare no competing financial interest.

■ ACKNOWLEDGMENTS

H.F., S.T., and T.D.A. are grateful to the European Research Council (ERC) AMPRO project no. 280221 for financial support.

■ REFERENCES

(1) Fortunato, E.; Barquinha, P.; Martins, R. Oxide Semiconductor Thin-Film Transistors: A Review of Recent Advances. *Adv. Mater.* **2012**, *24*, 2945–2986.

(2) Sun, Y.; Seo, J. H.; Takacs, C. J.; Seifter, J.; Heeger, A. J. Inverted Polymer Solar Cells Integrated with a Low-Temperature-Annealed Sol-Gel-Derived ZnO Film as an Electron Transport Layer. *Adv. Mater.* **2011**, *23*, 1679–1683.

(3) Kim, H.; Horwitz, J. S.; Kushto, G. P.; Kafafi, Z. H.; Chrisey, D. B. Indium Tin Oxide Thin Films Grown on Flexible Plastic Substrates by Pulsed-laser Deposition for Organic Light-Emitting Diodes. *Appl. Phys. Lett.* **2001**, *79*, 284–286.

(4) Weiher, R. L. Electrical Properties of Single Crystals of Indium Oxide. *J. Appl. Phys.* **1962**, *33*, 2834–2839.

(5) Nomura, K.; Ohta, H.; Takagi, A.; Kamiya, T.; Hirano, M.; Hosono, H. Room-Temperature Fabrication of Transparent Flexible Thin-Film Transistors Using Amorphous Oxide Semiconductors. *Nature* **2004**, *432*, 488–492.

(6) Xirouchaki, C.; Kiriakidis, G.; Pedersen, T. F.; Fritzsche, H. Photoreduction and Oxidation of as-Deposited Microcrystalline Indium Oxide. *J. Appl. Phys.* **1996**, *79*, 9349–9352.

(7) Lavareda, G.; Nunes de Carvalho, C.; Fortunato, E.; Ramos, A. R.; Alves, E.; Conde, O.; Amaral, A. Transparent Thin Transistors Based on Indium Oxide Semiconductor. *J. Non-Cryst. Solids* **2006**, *352*, 2311–2314.

(8) Gupta, R. K.; Mamidi, N.; Ghosh, K.; Mishra, S. R.; Kahol, P. K. Growth and Characterization of In_2O_3 Thin Films Prepared by Pulsed Laser Deposition. *J. Optoelectron. Adv. Mater.* **2007**, *9*, 2211–2216.

(9) Lee, J. S.; Kwack, Y.-J.; Choi, W.-S. Inkjet-Printed In_2O_3 Thin-Film Transistor below 200 °C. *ACS Appl. Mater. Interfaces* **2013**, *5*, 11579–11583.

(10) Siefert, W. Properties of Thin In_2O_3 and SnO_2 Films Prepared by Corona Spray Pyrolysis, and a Discussion of the Spray Pyrolysis Process. *Thin Solid Films* **1984**, *120*, 275–282.

(11) Patil, P. S. Versatility of Chemical Spray Pyrolysis Technique. *Mater. Chem. Phys.* **1999**, *59*, 185–198.

(12) Bashir, A.; Wöbkenberg, P. H.; Smith, J.; Ball, J. M.; Adamopoulos, G.; Bradley, D. D. C.; Anthopoulos, T. D. High-Performance Zinc Oxide Transistors and Circuits Fabricated by Spray Pyrolysis in Ambient Atmosphere. *Adv. Mater.* **2009**, *21*, 2226–2231.

(13) Adamopoulos, G.; Thomas, S.; Bradley, D. D. C.; McLachlan, M. A.; Anthopoulos, T. D. Low-Voltage ZnO Thin-Film Transistors Based on Y_2O_3 and Al_2O_3 High-κ Dielectrics Deposited by Spray Pyrolysis in Air. *Appl. Phys. Lett.* **2011**, *98*, 123503.

(14) Adamopoulos, G.; Thomas, S.; Wöbkenberg, P. H.; Bradley, D. D. C.; McLachlan, M. A.; Anthopoulos, T. D. High-Mobility Low-Voltage ZnO and Li-Doped ZnO Transistors Based on ZrO_2 High-κ Dielectric Grown by Spray Pyrolysis in Ambient Air. *Adv. Mater.* **2011**, *23*, 1894−1898.
(15) Faber, H.; Butz, B.; Dieker, C.; Spiecker, E.; Halik, M. Fully Patterned Low-Voltage Transparent Metal Oxide Transistors Deposited Solely by Chemical Spray Pyrolysis. *Adv. Funct. Mater.* **2013**, *23*, 2828−2834.
(16) Ortel, M.; Trostyanskaya, Y. S.; Wagner, V. Spray Pyrolysis of ZnO−TFTs Utilizing a Perfume Atomizer. *Solid-State Electron.* **2013**, *86*, 22−26.
(17) Pasquarelli, R. M.; Ginley, D. S.; O'Hayre, R. Solution Processing of Transparent Conductors: From Flask to Film. *Chem. Soc. Rev.* **2011**, *40*, 5406−5441.
(18) Kim, H. S.; Byrne, P. D.; Facchetti, A.; Marks, T. J. High Performance Solution-Processed Indium Oxide Thin-Film Transistors. *J. Am. Chem. Soc.* **2008**, *130*, 12580−12581.
(19) Han, S.-Y.; Herman, G. S.; Chang, C.-h. Low-Temperature, High-Performance, Solution-Processed Indium Oxide Thin-Film Transistors. *J. Am. Chem. Soc.* **2011**, *133*, 5166−5169.
(20) Manoj, P. K.; Gopchandran, K. G.; Koshy, P.; Vaidyan, V. K.; Joseph, B. Growth and Characterization of Indium Oxide Thin Films Prepared by Spray Pyrolysis. *Opt. Mater.* **2006**, *28*, 1405−1411.
(21) Bagheri Khatibani, A.; Abdolahzadeh Ziabari, A.; Rozati, S. M.; Bargbidi, Z.; Kiriakidis, G. Characterization and Gas-Sensing Performance of Spray Pyrolysed In_2O_3 Thin Films: Substrate Temperature Effect. *Trans. Electr. Electron. Mater.* **2012**, *13*, 111−115.
(22) Korotcenkov, G.; Brinzari, V.; Cerneavschi, A.; Ivanov, M.; Golovanov, V.; Cornet, A.; Morante, J.; Cabot, A.; Arbiol, J. The Influence of Film Structure on In_2O_3 Gas Response. *Thin Solid Films* **2004**, *460*, 315−323.
(23) Joseph Prince, J.; Ramamurthy, S.; Subramanian, B.; Sanjeeviraja, C.; Jayachandran, M. Spray Pyrolysis Growth and Material Properties of In_2O_3 Films. *J. Cryst. Growth* **2002**, *240*, 142−151.
(24) Girtan, M.; Folcher, G. Structural and Optical Properties of Indium Oxide Thin Films Prepared by an Ultrasonic Spray CVD Process. *Surf. Coat. Technol.* **2003**, *172*, 242−250.
(25) Raj, M. E.; Lalithambika, A.; Vidhya, K. C.; Rajagopal, V. S.; Thayumanavan, G.; Jayachandran, A.; Sanjeeviraja, M.; Growth, C. Mechanism and Optoelectronic Properties of Nanocrystalline In_2O_3 Films Prepared by Chemical Spray Pyrolysis of Metal-Organic Precursor. *Physica B* **2008**, *403*, 544−554.
(26) Kim, M.-G.; Kanatzidis, M. G.; Facchetti, A.; Marks, T. J. Low-Temperature Fabrication of High-Performance Metal Oxide Thin-Film Electronics via Combustion Processing. *Nat. Mater.* **2011**, *10*, 382−388.
(27) Park, J. H.; Yoo, Y. B.; Lee, K. H.; Jang, W. S.; Oh, J. Y.; Chae, S. S.; Lee, H. W.; Han, S. W.; Baik, H. K. Boron-Doped Peroxo-Zirconium Oxide Dielectric for High-Performance, Low-Temperature, Solution-Processed Indium Oxide Thin-Film Transistor. *ACS Appl. Mater. Interfaces* **2013**, *5*, 8067−8075.
(28) Hwan Hwang, Y.; Seo, J.-S.; Moon Yun, J.; Park, H.; Yang, S.; Ko Park, S.-H.; Bae, B.-S. An Aqueous Route for the Fabrication of Low-Temperature-Processable Oxide Flexible Transparent Thin-Film Transistors on Plastic Substrates. *NPG Asia Mater.* **2013**, *5*, e45.
(29) Ortel, M.; Wagner, V. Leidenfrost Temperature Related CVD-like Growth Mechanism in ZnO-TFTs Deposited by Pulsed Spray Pyrolysis. *J. Cryst. Growth* **2013**, *363*, 185−189.
(30) Krunks, M.; Mellikov, E. Zinc Oxide Thin Films by the Spray Pyrolysis Method. *Thin Solid Films* **1995**, *270*, 33−36.
(31) Jothibas, M.; Manoharan, C.; Ramalingam, S.; Dhanapandian, S.; Johnson Jeyakumar, S.; Bououdina, M. Preparation, Characterization, Spectroscopic (FT-IR, FT-Raman, UV and Visible) Studies, Optical Properties and Kubo Gap Analysis of In_2O_3 Thin Films. *J. Mol. Struct.* **2013**, *1049*, 239−249.
(32) Weiher, R. L.; Ley, R. P. Optical Properties of Indium Oxide. *J. Appl. Phys.* **1966**, *37*, 299−302.
(33) Sinha, S. K.; Sirota, E. B.; Garoff, S.; Stanley, H. B. X-ray and Neutron Scattering from Rough Surfaces. *Phys. Rev. B* **1988**, *38*, 2297−2311.
(34) Patsalas, P.; Logothetidis, S.; Kelires, P. C. Surface and Interface Morphology and Structure of Amorphous Carbon Thin and Multilayer Films. *Diamond Relat. Mater.* **2005**, *14*, 1241−1254.
(35) Panagiotopoulos, N. T.; Diamanti, E. K.; Koutsokeras, L. E.; Baikousi, M.; Kordatos, E.; Matikas, T. E.; Gournis, D.; Patsalas, P. Nanocomposite Catalysts Producing Durable, Super-Black Carbon Nanotube Systems: Applications in Solar Thermal Harvesting. *ACS Nano* **2012**, *6*, 10475−10485.
(36) Wanger, C. D.; Riggs, W. M.; Davis, L. E.; Moulder, J. F.; Muilenberg, G. E. *Handbook of X-ray Photoelectron Spectroscopy*; Perkin-Elmer Corp. Physical Electronics Division: Eden Prairie, MN, 1979.
(37) Purvis, K. L.; Lu, G.; Schwartz, J.; Bernasek, S. L. Surface Characterization and Modification of Indium Tin Oxide in Ultrahigh Vacuum. *J. Am. Chem. Soc.* **2000**, *122*, 1808−1809.
(38) Yin, W.; Esposito, D. V.; Yang, S.; Ni, C.; Chen, J. G.; Zhao, G.; Zhang, Z.; Hu, C.; Cao, M.; Wei, B. Controlling Novel Red-Light Emissions by Doping In_2O_3 Nano/Microstructures with Interstitial Nitrogen. *J. Phys. Chem. C* **2010**, *114*, 13234−13240.
(39) Lin, Y.-H.; Faber, H.; Zhao, K.; Wang, Q.; Amassian, A.; McLachlan, M.; Anthopoulos, T. D. High-Performance ZnO Transistors Processed via an Aqueous Carbon-Free Metal Oxide Precursor Route at Temperatures between 80−180 °C. *Adv. Mater.* **2013**, *25*, 4340−4346.

DOI: 10.1021/am5072139
ACS Appl. Mater. Interfaces 2015, 7, 782−790